Chapter 3

Wireless Power Transfer by Using Magnetically Coupled Resonators

Ali Agcal, Selin Ozcira and Nur Bekiroglu

Additional information is available at the end of the chapter

http://dx.doi.org/10.5772/64031

Abstract

In this chapter, a wireless power transmission system based on magnetic resonance coupling circuit was carried out. Mathematical expressions of optimal coupling coefficients were examined with the coupling model. Equivalent circuit parameters were calculated with Maxwell 3D software, and then, the equivalent circuit was solved using MATLAB technical computing software. The transfer efficiency of the system was derived using the electrical parameters of the equivalent circuit. System efficiency was analyzed depending on the different air gap values for various characteristic impedances using PSIM circuit simulation software. Since magnetic resonance coupling involves creating a resonance and transferring the power without the radiation of electromagnetic waves, resonance frequency is a key parameter in system design. The aim of this research was to define the efficiency according to variations of coefficients in wireless power transfer (WPT) system. In order to do that, the calculation procedure of mutual inductance between two self-resonators is performed by Maxwell software. Equivalent circuit is solved in circuit simulator PSIM platform. The calculations show that using the parameters that are obtained by magnetic analysis can be used for the equivalent circuit which has the capability to provide the efficiency using electrical quantities. The chapter discusses the application of this approach to a coil excited by a sinusoidal voltage source and a receiver coil, which receives energy voltage and current. Both could be obtained to calculate the instantaneous power and efficiency. To do so, the waveforms for voltage and current were obtained and computed with the PSIM circuit simulator. As the air gap between the coils increased, the coupling between the coils was weakened. The impedance of the circuit varied as the air gap changed, affecting the power transfer efficiency. In order to determine the differences between the software programs, efficiency values were calculated using three kinds of software. And it is concluded that equivalent circuit analysis by means of numerical computing is proper to obtain the voltage and current waveforms. Correspondingly, transmission efficiency can be calculated using the electrical relations.

Keywords: wireless power transfer, magnetically coupling resonators, efficiency variations

1. Introduction

Wireless power transfer (WPT) has become popular recently and is expected to be used in plenty of technological devices. The main reason for the recent intense interest in WPT is the sharp increase in the use of electrical devices with various sizes and types of batteries. The main purpose of WPT research was the transfer of as much power as possible, with the goal of high system efficiency in spite of low mutual inductance between coils.

In the literature, one of the popular publications that take range variations into consideration is [1]. Critical coupling, frequency splitting, and impedance matching issues were analyzed in [1] using single-turn axillary loops to amplify the magnetic coupling added to resonators. In [1], the authors revealed 50% efficiency for their system, which is suitable for various positions of the receiver.

It has become widely accepted to use a series resonating circuit as the equivalent circuit of a resonator to conduct analysis for resonant frequency [2]. In this context, different attempts have been made to develop a sufficiently precise model [3,4]. There have been many methods employed such as modification circuits and magnetic design of the core properties [5]. In those studies, the scattering parameters were calculated by two port network theory using a network analyzer.

The state space model was created to obtain an accurate mathematical model of wireless power transfer (WPT) in [6,7], in which the transfer function of the bidirectional IPT system was obtained. As the Ziegler–Nichols method has high overshoot, it was optimized the PID parameters with a phase margin of 60° [8]. The PID parameters were optimized using the genetic algorithm in order to achieve better transient performance in [9]. The dynamic behavior ought to be as fast as possible in [10], in which the H-bridge circuit structure was inserted into the dynamic model. In [11], authors proposed a dynamic model for a multi-pickup system. To overcome the higher order problem and make a straightforward real dynamic model from the energy point of view, it was built a dynamic model of the WPT including a nonlinear inverter and rectifier in [12].

In [13], authors proposed a design methodology using a series-series (S-S) contactless power transfer system for an EV battery charger with two fixed operating frequencies. The converter operates at one of the fixed frequencies for a load-independent current output and at the other operating frequency for a load-independent voltage output. It was proposed hybrid topologies using either SS and PS compensation or SP and PP compensation for battery charging [14]. Controlling output current or voltage is achieved with two different methods. One is PWM (Pulse width modulation) control at a constant frequency at which huge changes in the duty

http://dx.doi.org/10.5772/64031

cycle will not allow zero voltage switching (ZVS) [15]. Cost analysis was performed in [16], and the results showed that coils are the most expensive part of the system.

System analysis in terms of electrical circuit is necessary since magnetic resonance coupling involves creating LC resonance. To derive the analytical equations of the input impedance and transferred power, a simplified circuit model of the WPT systems can be used. In order to calculate parameters such as current and voltage as a function of frequency at various air gap values and load conditions, mutual inductance between two self-resonators can be obtained from magnetic circuit analysis. And the parameters that are obtained by magnetic analysis can be used to solve the equivalent circuit which makes it possible to calculate the efficiency using electrical relations.

2. Magnetic resonance circuit

Resonance is observed in many different ways in nature. In general, resonance denotes the oscillation of energy between two different modes. For example, a mechanical pendulum oscillates between potential and kinetic forms of energy. While a system is in resonance, a huge amount of energy can be store with lower excitation. If the energy intake speed ratio of the system is larger than the energy loss ratio of the system, energy accumulation occurs.

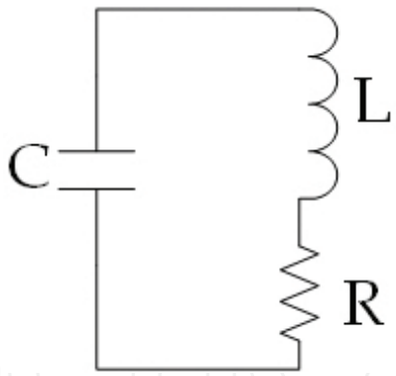

Figure 1. Resonator.

An example of an electro-magnetic resonator circuit with a coil, a capacitor, and a resistor is shown in **Figure 1**.

In this circuit, the energy oscillates between the coil (which stores energy in the magnetic field) and capacitors (which store energy in an electric field) at a certain resonance frequency.

$$\omega_0 = \frac{1}{\sqrt{LC}} \tag{1}$$

$$Q = \sqrt{\frac{L}{C}}\frac{1}{R} = \frac{\omega_0 L}{R} \tag{2}$$

From Eq. (2), it can be seen that the quality factor of the system increases, decreasing the circuit loss (the reduction of R).

In a high-resonance wireless power transfer system, the resonator system must have a high quality factor for efficient energy transfer. High quality factor electromagnetic resonators are normally made from the conductive components which have relatively narrow resonant frequency widths. The resonance frequency range is narrow, and resonators can be designed to reduce their interactions with foreign objects.

If two resonators are placed close to one another, the resonators can form a link and will be able to exchange energy. The efficiency of the energy exchange varies depending on each resonator and the coupling ratio k. The dynamics of a system with two resonators can be identified from the coupling mode theory or from equivalent circuit analysis of the connection system for the resonator. The equivalent circuit for coupled resonators has a series resonance circuit structure as shown in **Figure 2**.

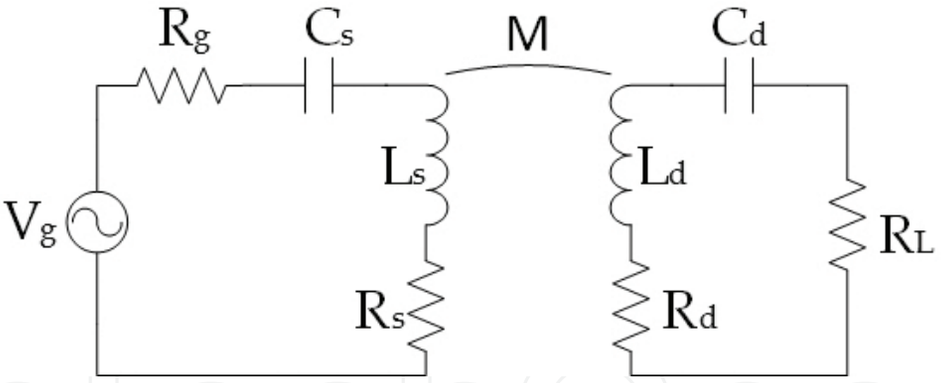

Figure 2. Equivalent circuit of coupled resonator system.

Here, R is the source internal resistance and the frequency is ω(2πf). Vg is called amplitude of the voltage source. L_s and L_d are source and device resonator coils, respectively. And mutual inductance is indicated by $M = k\sqrt{L_s L_d}$. Each coil has a series capacitor that forms a resonator. R_s and R_d resistors denote unwanted resistance (including ohmic and radiation losses) in the coil and the resonance capacitor for each resonator. AC load resistance is shown as R_L.

The yield for this circuit can be determined from the ratio of transmitted power for load resistance to the maximum available power of the source, while resonator system is strongly coupled.

http://dx.doi.org/10.5772/64031

$$\frac{P_L}{P_{g,max}} = \frac{4U^2 \frac{R_g}{R_s}\frac{R_L}{R_d}}{\left[\left(1+\frac{R_g}{R_s}\right)\left(1+\frac{R_L}{R_d}\right)+U^2\right]^2} \tag{3}$$

$$U = \frac{\omega M}{\sqrt{R_s R_d}} = k\sqrt{Q_s Q_d} \tag{4}$$

To provide the best system performance, proper load and source resistance can be selected or other resistance values can be captured using an impedance matching link. If the resistance is selected using Eq. (5),

$$\frac{R_g}{R_s} = \frac{R_L}{R_d} = \sqrt{1+U^2} \tag{5}$$

power transfer efficiency can be expressed by Eq. (6)

$$\eta_{opt} = \frac{U^2}{\left(1+\sqrt{1+U^2}\right)^2} \tag{6}$$

Using Eq. (6), the maximum power transmission efficiency can be depicted as in **Figure 3**.

Systems with large values of U can achieve highly efficient energy transfer. Best wireless energy transfer system efficiency can be possible by determining the performance factors of the system, such as U which is depend on magnetic coupling coefficient k, and quality factors of the Q_s (source) and Q_d (device).

For certain applications, the resonator quality factor and magnetic coupling between resonators are used to determine the best possible performance for the system.

For wireless power transfer, it can be seen in Eq. (4) that the magnetic coupling coefficient and quality factor of the significance is greater. The magnetic coupling coefficient represents the magnetic flux connection between the source, while the device resonator is a dimensionless parameter with a value between 0 (unconnected) and 1 (complete flux linked). Conventional induction-based wireless power transmission systems (such as electric toothbrushes) have a high coupling value and a close range, aligned between the source and the device. Eq. (4) indicates that a high-quality resonator is more efficient than a traditional induction system. More importantly, it becomes possible to work efficiently at low coupling values. Also, for this reason, the need for precise positioning between the source and the device is eliminated. Unfortunately, the biggest drawback of the high quality factor is that the capacitor's peak

voltage is too high. The relationship between the peak value of the capacitor voltage and the quality is shown in Eq. (7) [17].

$$V_{Cpeak} = Q\frac{2V_s}{\pi} \tag{7}$$

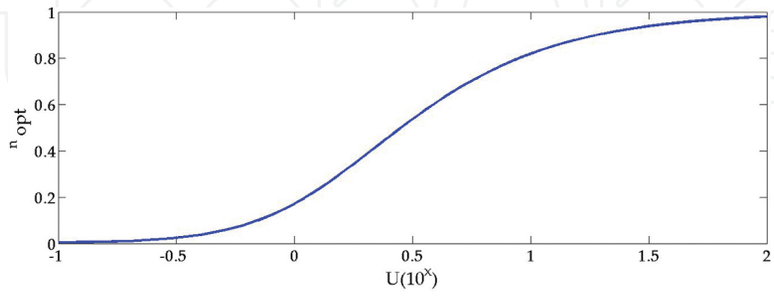

Figure 3. Depending on the U function, the optimum efficiency graph of energy transfer.

2.1. Magnetic coupling circuit

$$V_1 = I_1\left(R + jL_1\omega + \left(\frac{1}{j\omega C}\right)\right) - I_2\left(jL_m\omega\right) \tag{8}$$

$$0 = I_2\left(jL_2\omega + \left(\frac{1}{j\omega C}\right) + Z_0 + R\right) - I_1\left(jL_m\omega\right) \tag{9}$$

$$I_2\left(jL_2\omega + \left(\frac{1}{j\omega C}\right) + Z_0 + R\right) = I_1\left(jL_m\omega\right) \tag{10}$$

$$I_2 = I_1\left(\frac{jL_m\omega}{jL_2\omega + \left(\frac{1}{j\omega C}\right) + Z_0 + R}\right) \tag{11}$$

$$V_1 = I_1\left(R + jL_1\omega + \left(\frac{1}{j\omega C}\right)\right) - I_1\left(\frac{jL_m\omega}{jL_2\omega + \left(\frac{1}{j\omega C}\right) + Z_0 + R}\right)\left(jL_m\omega\right) \tag{12}$$

http://dx.doi.org/10.5772/64031

$$V_1 = I_1\left[\left(R + jL_1\omega + \left(\frac{1}{j\omega C}\right)\right) - \left(\frac{j^2 {L_m}^2\omega^2}{jL_2\omega + \left(\frac{1}{j\omega C}\right) + Z_0 + R}\right)\right] \tag{13}$$

$$Z_{Eq} = Z_i = R + jL_1\omega + \left(\frac{1}{j\omega C}\right) + \left(\frac{{L_m}^2\omega^2}{jL_2\omega + \left(\frac{1}{j\omega C}\right) + Z_0 + R}\right) \tag{14}$$

$$Z_{Eq} = R + jL_1\omega + \left(\frac{1}{j\omega C}\right) + \left(\frac{{L_m}^2\omega^2}{jL_2\omega + \left(\frac{1}{j\omega C}\right) + Z_0 + R}\right) + jL_m\omega - jL_m\omega \tag{15}$$

$$Z_{Eq} = R + \left(\frac{1}{j\omega C}\right) + j(L_1 - L_m)\omega + \frac{-j^2{L_m}^2\omega^2 + j^2L_mL_2\omega^2 + jL_m\omega(Z_0 + R) + jL_m\left(\frac{1}{j\omega C}\right)\omega}{jL_2\omega + \left(\frac{1}{j\omega C}\right) + Z_0 + R} \tag{16}$$

$$Z_{Eq} = R + \left(\frac{1}{j\omega C}\right) + j(L_1 - L_m)\omega + \frac{(jL_m\omega)\left(j(L_2 - L_m)\omega + \left(\frac{1}{j\omega C}\right) + Z_0 + R\right)}{jL_2\omega + \left(\frac{1}{j\omega C}\right) + Z_0 + R} \tag{17}$$

$$Z_{Eq} = R + \left(\frac{1}{j\omega C}\right) + j(L_1 - L_m)\omega + \frac{1}{\frac{jL_2\omega + \left(\frac{1}{j\omega C}\right) + Z_0 + R + jL_m\omega - jL_m\omega}{(jL_m\omega)\left(j(L_2 - L_m)\omega + \left(\frac{1}{j\omega C}\right) + Z_0 + R\right)}} \tag{18}$$

$$Z_{Eq} = R + \left(\frac{1}{j\omega C}\right) + j(L_1 - L_m)\omega + \frac{1}{\frac{1}{jL_m\omega} + \frac{1}{j(L_2 - L_m)\omega + (1/\ j\omega C) + Z_0 + R}} \tag{19}$$

Since voltage and current are electrical quantities, the voltage equation can be written in a manner that calculates the electrical efficiency [18]. This leads to a set of equivalent impedance equations. The equivalent impedance is obtained by (19). Assuming $C = C_1 = C_2$ in the resonance coupling system, the efficiency can be defined by (22).

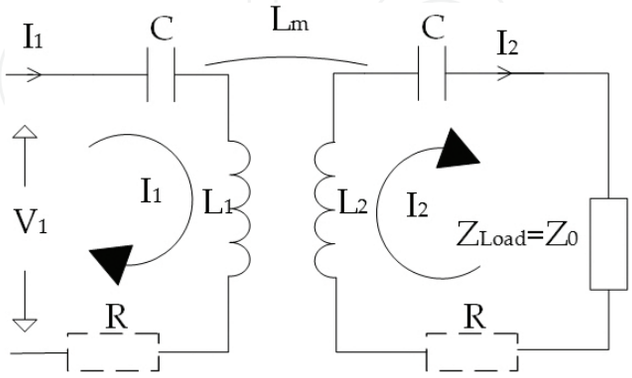

Figure 4. Magnetic coupling circuit.

2.2. Efficiency equation

$$\eta = \frac{P_{out}}{P_{in}} = \frac{I_{out}^2 Z_{out}}{I_{in}^2 Z_{Eq}} \tag{20}$$

Eq. (11) makes use of (21);

$$\frac{I_{out}}{I_{in}} = \frac{jL_m\omega}{jL_2\omega + \left(\frac{1}{j\omega C}\right) + Z_0 + R} \tag{21}$$

Eqs. (21) and (14) are substituted for Eq. (20);

$$\eta = \left(\frac{jL_m\omega}{jL_2\omega + \left(\frac{1}{j\omega C}\right) + Z_0 + R}\right)^2 \frac{Z_0}{\left(R + jL_1\omega + \left(\frac{1}{j\omega C}\right) + \left(\frac{{L_m}^2\omega^2}{jL_2\omega + \left(\frac{1}{j\omega C}\right) + Z_0 + R}\right)\right)} \tag{22}$$

At a given resonant frequency, the conditions for system efficiency are defined for three states, defined by Eqs. (23), (24), and (25).

http://dx.doi.org/10.5772/64031

$$L_m^2 = \frac{Z_0^2 - R^2}{\omega_0^2} \tag{23}$$

$$L_m^2 > \frac{Z_0^2 - R^2}{\omega_0^2} \tag{24}$$

$$L_m^2 < \frac{Z_0^2 - R^2}{\omega_0^2} \tag{25}$$

Eq. (23) describes the maximum efficiency condition, while Eq. (24) represents the double resonance frequency condition. Eq.(25) describes the condition of the system with a single-resonant frequency at low efficiency level [19].

3. Efficiency and characteristic impedance variation simulations with different software tools

Resonance frequency is a key parameter in system design, and the value can be changed by adjusting the distance between the transmission and characteristic impedance of the electrical circuit. First, the electrical circuit is created in a PSIM circuit simulator and the resulting voltage and current waveforms are obtained via the simulator. PSIM is simulation software designed for power electronics, motor control, and dynamic system simulation. The simulation is solved in the Matlab platform, and a procedure to calculate the parameters of the equivalent circuit is performed in Maxwell. For an air gap of 10 cm L = 999.2nH, C = 124pF, L_m = 128.6H, Z_0 = 5Ω, the efficiency chart and variations in the equivalent impedance chart are given in **Figures 5** and **6**, respectively.

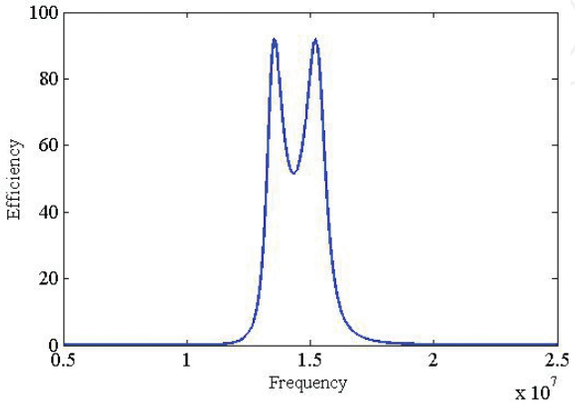

Figure 5. Efficiency chart.

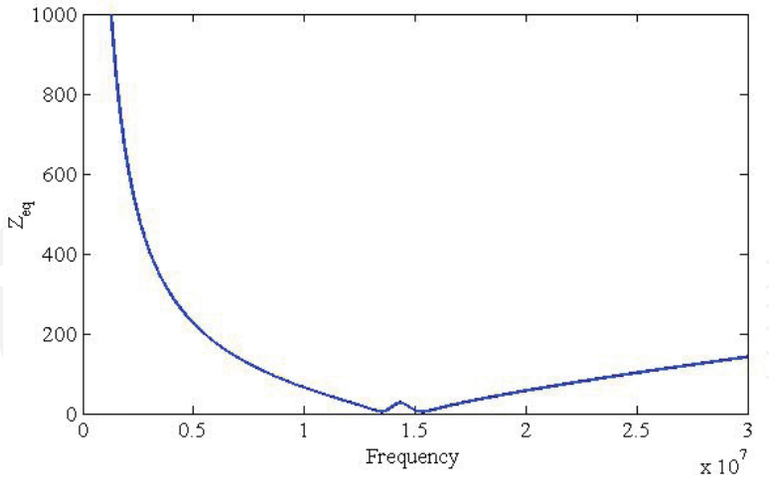

Figure 6. Equivalent impedance chart.

The transmitter and receiver coils have four different resonance coupling states: In the first state, both the transmitter and receiver coil loops are not resonant; in the second, the transmitter coil loop is in resonance, while the receiver coil loop is not; in the third, the transmitter coil loop is not resonant, while the receiver coil is; and in the last state, both the transmitter and receiver coil loops are resonant. When the whole coupling system is in resonance, the impedance value is at a minimum.

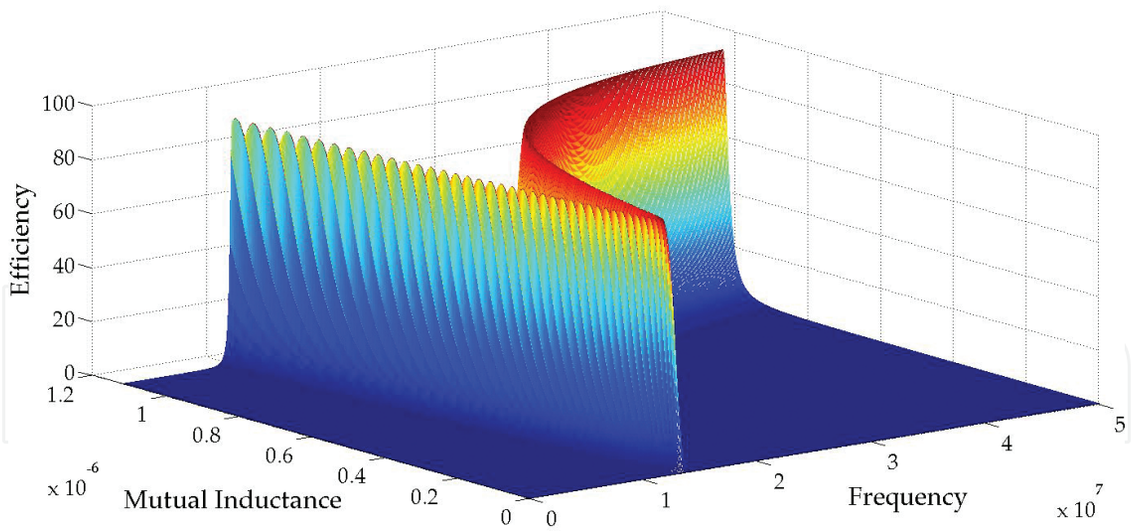

Figure 7. Function of efficiency according to mutual inductance and frequency.

The resonant frequencies change from two points to one depending on the length of the air gap. The double-resonance frequency region occurs at low impedance and short range. As the air gap distance and impedance increase, one resonance region appears. At this operation range, the efficiency falls sharply. The critical transmission efficiency would be the same as the peak efficiency over a coupled range.

http://dx.doi.org/10.5772/64031

The distance between the coils responsible for energy transfer should be kept at an optimum value since any increase in the air gap value will degrade the energy transfer ratio. This problem can be solved by optimizing the relation between the frequency and the quality factor.

Calculation of the parameters for the equivalent circuit was carried out in the Maxwell 3D software platform as well as in PSIM.

3.1. Maxwell 3D software simulation results

Hundred volts were used for the ideal sine source of 13.552 MHz. An inductance of winding value of 999.2 nH, mutual inductance of 128.6 nH, 124 pF capacitor values, R value of 0.22 Ω, and Z_0 impedance value of 5 Ω were selected. The circuit scheme and modeled coils can be seen from **Figures 8** and **9**. The magnetic flux density graphs and waveforms of currents and voltage for air gap of 10 cm can be seen from **Figures 10–14**.

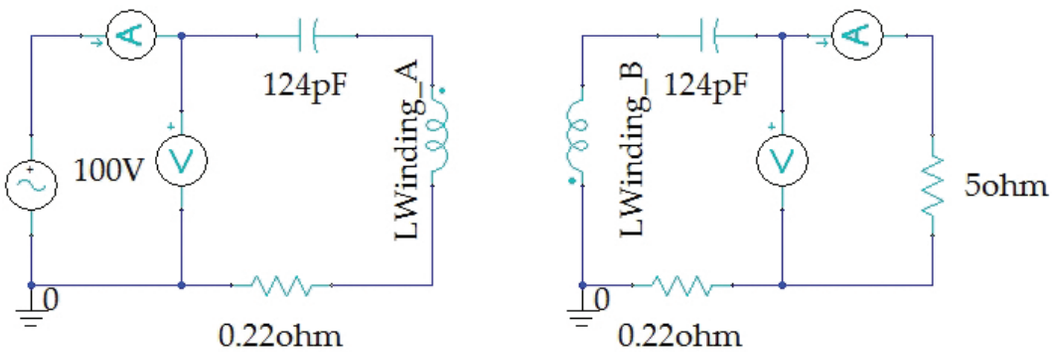

Figure 8. Maxwell 3D circuit scheme.

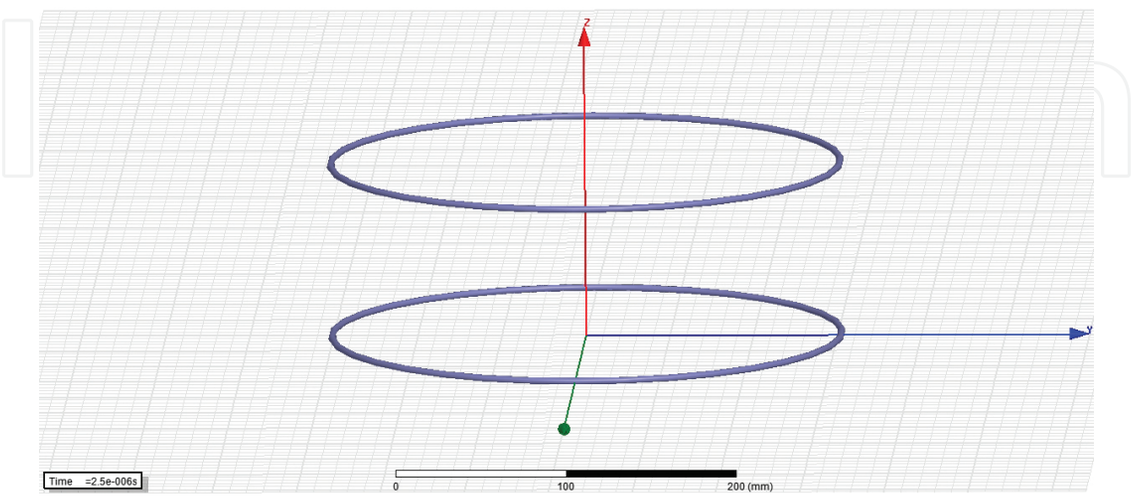

Figure 9. Receiver and transmitter coil for 10-cm air gap in Maxwell 3D.

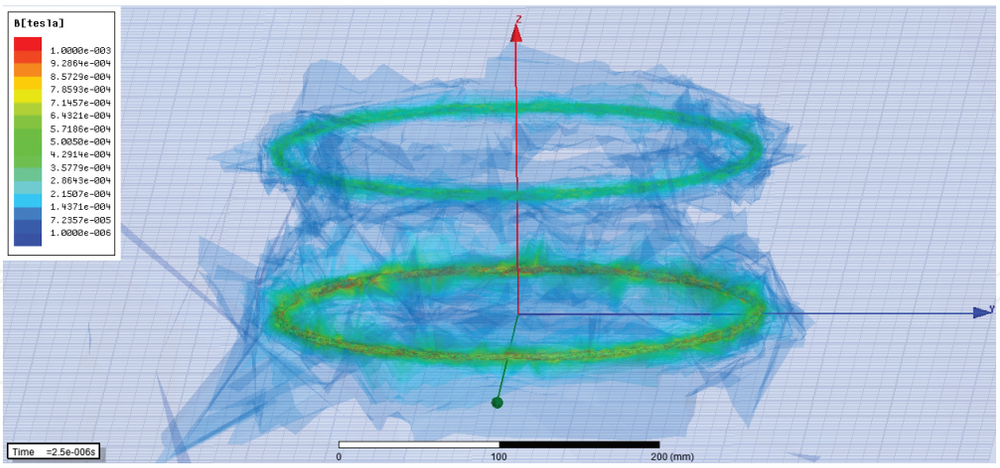

Figure 10. Magnetic flux density of receiver and transmitter coil for 10-cm air gap in Maxwell 3D.

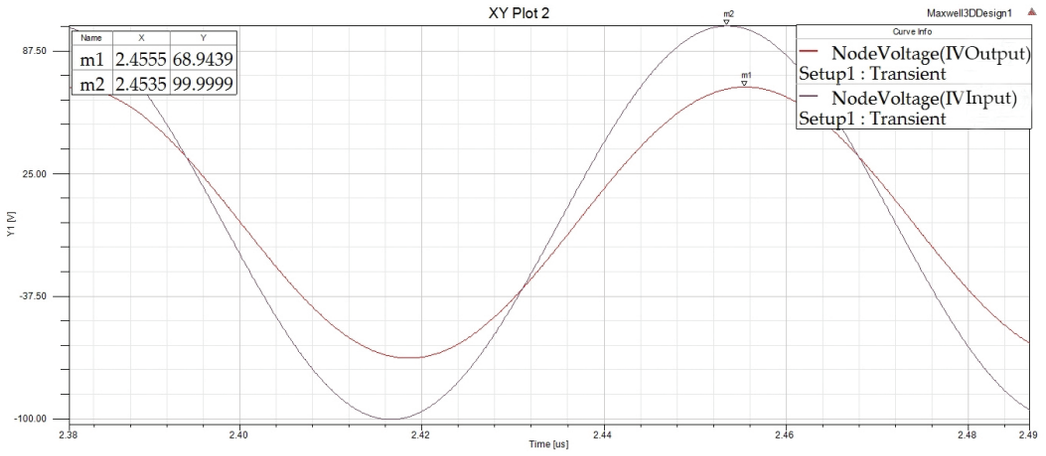

Figure 11. Maxwell 3D input and output voltages for 10-cm air gap and characteristic impedance of 5 Ω.

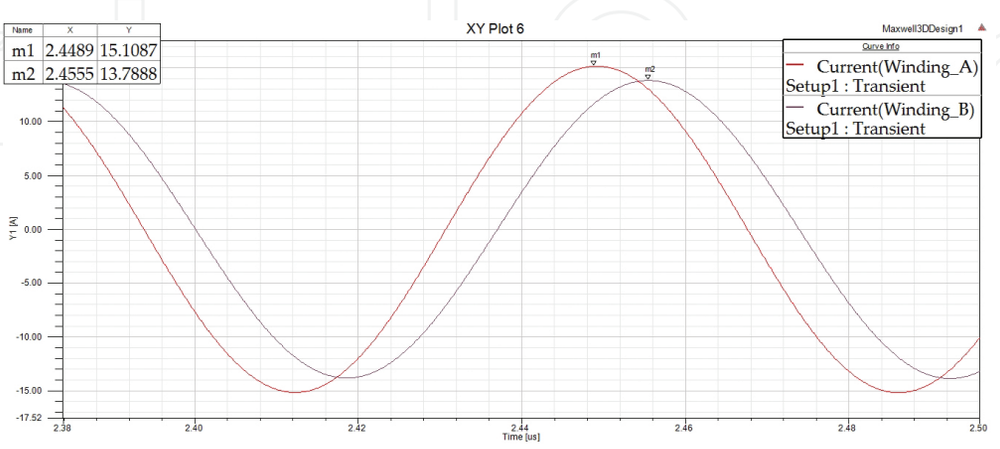

Figure 12. Maxwell 3D current passing through primary and secondary windings.

http://dx.doi.org/10.5772/64031

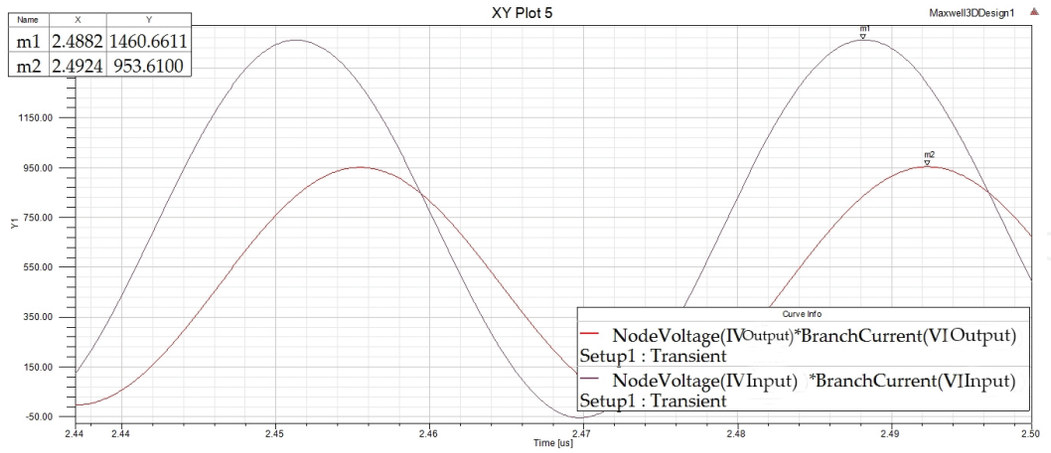

Figure 13. Maxwell 3D input and output power for 10-cm air gap and characteristic impedance of 5 Ω.

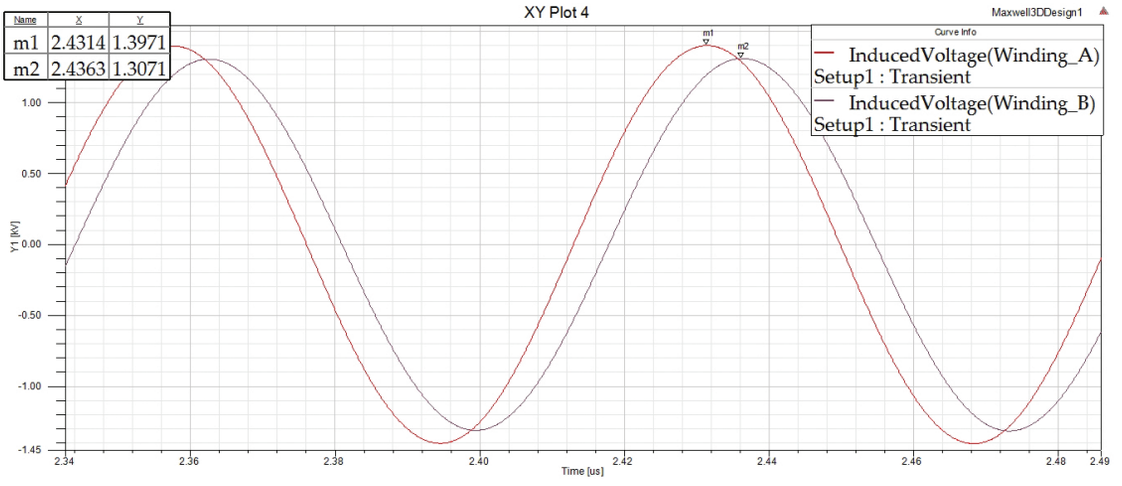

Figure 14. Maxwell 3D primary and secondary winding terminal voltage for 10-cm air gap and the characteristic impedance of 5 Ω.

3.2. PSIM software simulation results

To determine the power and efficiency, the previously described methodology was followed. First, the mean required values for the circuit parameters for the Maxwell field simulator were computed. In the circuit simulation, the wireless power transfer system is driven by a sinusoidal voltage source with amplitude of 100 V. **Figure 15** shows the structure of the direct fed wireless power transfer. In order to illustrate how the model works, transient simulations were performed with the PSIM circuit simulator.

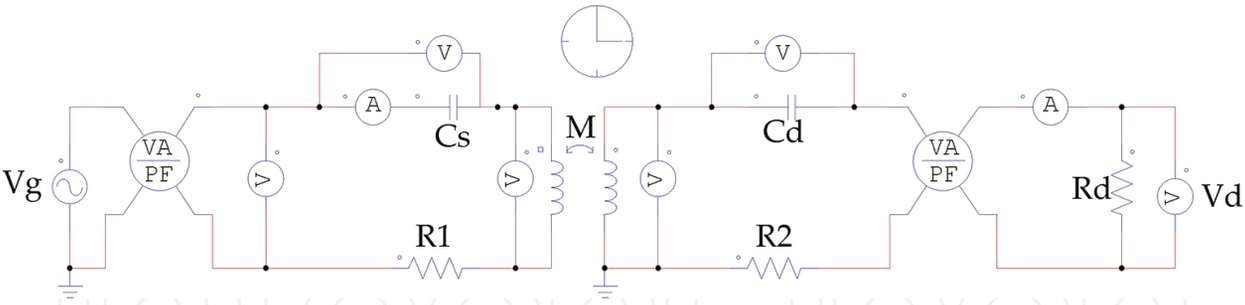

Figure 15. PSIM circuit scheme.

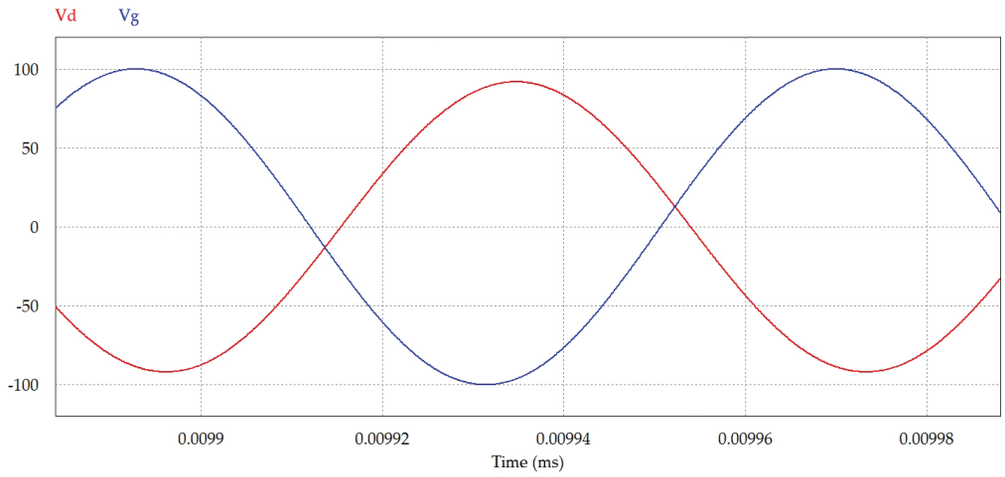

Figure 16. Air gap of 10 cm, characteristic impedance of 5 Ω at 13.56 MHz input voltage (VP1 red line) and device voltage waveforms (VP2 blue line).

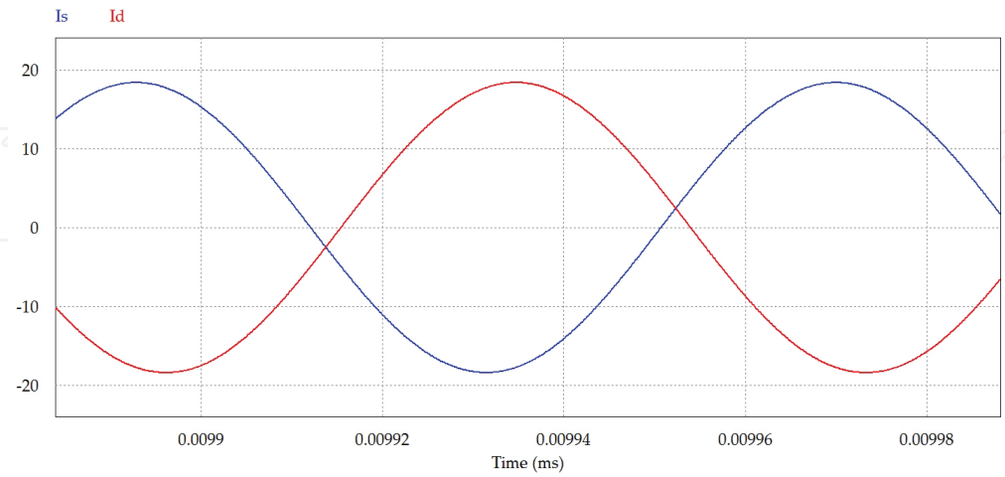

Figure 17. Air gap of 10 cm, characteristic impedance of 5 Ω at 13.56 MHz input current (VP1 red line) and device input waveforms (VP2 blue line).

http://dx.doi.org/10.5772/64031

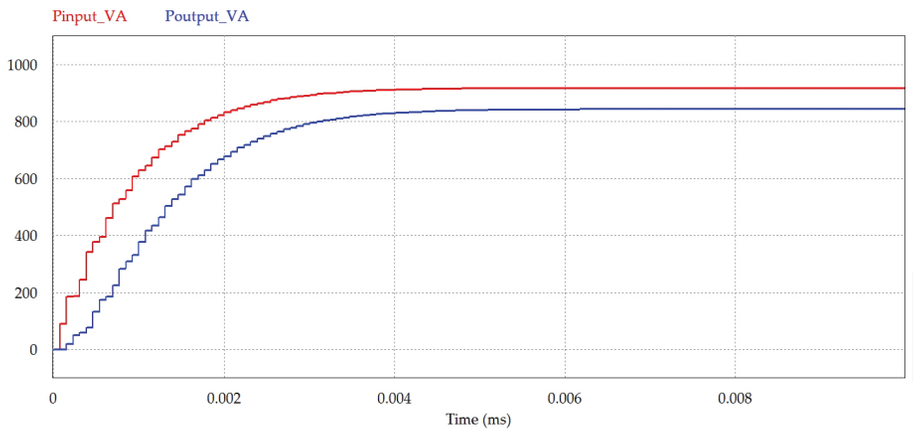

Figure 18. Air gap of 10 cm, characteristic impedance of 5 Ω at 13.56 MHz (blue: input power, red: received power).

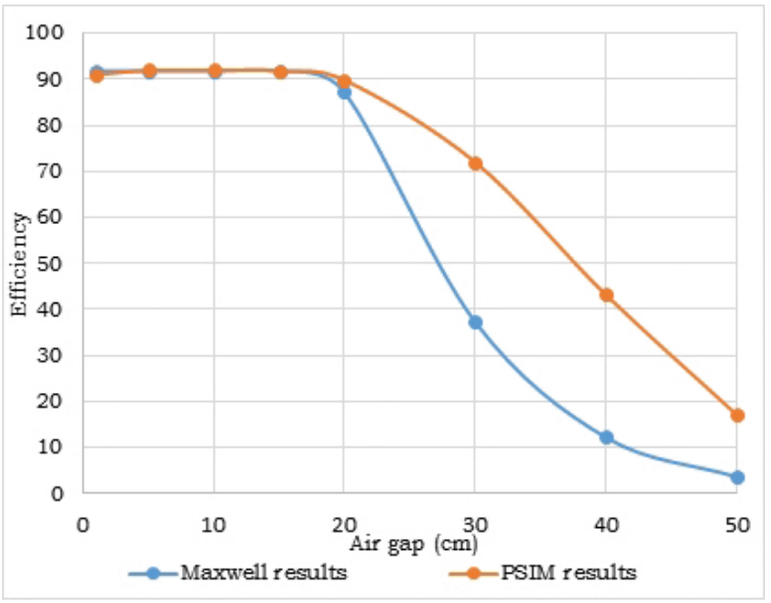

Figure 19. Magnetic resonance efficiencies according to software platforms.

The transmitting current was 13 A, and the receiving current was 12.88 A for a supply voltage of 70.71 V and the device voltage below 65 V. When input power was 919.2 VA, the amount of power delivery is 837 VA. Approximately 82.2 VA dissipated for losses and the transmitter required 0.098 W (an overhead loss) plus an additional input power of 1.098 VA for every additional 1 VA of power at the receiver.

When the same simulations run on Maxwell and PSIM software platforms for various air gap values, it is observed that for strongly magnetic coupled range up to air gap of 10 cm, efficiency values can be obtained similar. However, if the magnetic coupling gets loosely by the effect of elongated air gap distance, efficiency value differs. The reason of that is the numerical solution method. Therefore, numerical computing such as circuit simulators can calculate the quantities for strongly magnetic resonance couplings.

4. Conclusion

In this study, analysis of voltage and current waveforms in terms of magnetic resonance coupling is performed using numerical computing and a circuit simulator to define the efficiency of wireless power transfer in the time domain. This approach takes into consideration the nonlinear effects of power losses. The numerical results based on various air gap values are determined from equivalent circuit parameters which are obtained directly from Maxwell by the results of method of moments electromagnetics analysis. The calculation of mutual inductance between two self-resonators is also performed using the Maxwell software, and the equivalent circuit is solved in the circuit simulator PSIM platform.

The aim of this research was to define the efficiency according to the coefficients of variations for the WPT system. The parameters of the system affect the coupling coefficient; Lm is the mutual inductance parameter, while L_1 and L_2 are nonlinear loss resistance values that depend on the frequency and characteristic impedance of the system. The results were validated using the finite element method.

We concluded that equivalent circuit analysis by means of numerical computing is appropriate for determining the voltage and current waveforms. Additionally, transmission efficiency at a different distance range can be calculated based on the electrical relationship. Efficiency results with respect to load variation show that there are double-resonance frequency regions as well as one-resonance region. The resonant frequencies change from two points to one point depending on the length of the air gap. The double-resonance frequency region occurs at low impedance and short range. As the air-gap distance and impedance increase, one resonance region appears. The efficiency falls sharply at this operation range.

Author details

Ali Agcal, Selin Ozcira* and Nur Bekiroglu

*Address all correspondence to: selinozcira@gmail.com

Department of Electrical Engineering, Yildiz Technical University, Istanbul, Turkey

References

[1] Sample A. P., Waters B. H., Wisdom S. T. and Smith J. R. Enabling seamless wireless power delivery in dynamic environments. Proc. IEEE. 2013;101(6):1343–1358. doi: 10.1109/JPROC.2013.2252453

[2] Wei W., Narusue Y., Kawahara Y., Kobayashi N., Fukuda H. and Tsukagoshi T. Characteristic analysis on double side spiral resonator's thickness effect on transmis-

sion efficiency for wireless power transmission. In: IEICE Tech. Committee Meeting; May 2012; Yokohama. IEICE; 2012. p. 1–5.

[3] Chih-Jung C., Tah-Hsiung C., Chih-Lung L. and Zeui-Chown J. A study of loosely coupled coils for wireless power transfer. IEEE Trans. Circ. Syst. II Express Briefs. 2010;57(7):536–540. doi:10.1109/TCSII.2010.2048403

[4] Kim Y. H., Kang S. Y., Lee M. L., Yu B. G. and Zyung T. Optimization of wireless power transmission through resonant coupling. In: Power electronics electrical drives automation and motion (SPEEDAM), 2010 international symposium; Sep. 2010; Pisa, Italy. USA: IEEE; 2009. p. 1069–1073. doi:10.1109/SPEEDAM.2010.5544862

[5] Salasa R. A. and Pleite J. Accurate modeling of voltage and current waveforms with saturation and power losses in a ferrite core via two-dimensional finite elements and a circuit simulator. J. Appl. Phys. 2010;107(9):1–4.

[6] Swain A. K., Neath M. J., Madawala U. K. and Thrimawithana D. J. A dynamic multivariable state-space model for bidirectional inductive power transfer syst.. IEEE. Trans. Power Electron. 2012;27(11):4772–4778.doi:10.1109/TPEL.2012.2185712

[7] Zahid Z. U., Dalala Z. and Lai J. Small signal modelling of series-series compensated induction power transfer system. In: IEEE 29th Annual Applied Power Electronic Conference Expo; Mar. 2014; Fort Worth, USA: IEEE; 2014. p. 2847–2853. doi:10.1109/APEC.2014.6803708

[8] Neath M. J., Swain A. K., Madawala U. K., Thrimawithana D. J. and Vilathgamuwa D. M. Controller synthesis of a bidirectional inductive power interface for electric vehicles. In: IEEE third international conference on sustainable energy technologies (ICSET; Sept. 2012; Kathmandu, Nepal). USA: IEEE; 2012. p. 60–65. doi:10.1109/ICSET.2012.6357376

[9] Neath M. J., Swain A. K., Madawala U. K. and Thrimawithana D. J. An optimal PID controller for a bidirectional inductive power transfer system using multiobjective genetic algorithm. IEEE. Trans. Power Electron. 2014;29(3):1523–1531.

[10] Hao H., Covic G. A. and Boys J. T. An approximate dynamic model of LCL-T-based inductive power transfer power supplies. IEEE Trans. Power Electron. 2014;29(10):5557–5567. doi:10.1109/TPEL.2013.2293138

[11] Swain A. K., Devarakonda S. and Madawala U. K. Modeling, sensitivity analysis, and controller synthesis of multipickup bidirectional inductive power transfer systems. IEEE Trans. Ind. Inf. 2014;10(2):1372–1380. doi:10.1109/TII.2014.2307159

[12] Li H., Wang K., Huang L., Chen W. and Yang X. Dynamic modeling based on coupled modes for wireless power transfer systems. IEEE Trans. Power Electron. 2015;30(11):6245–6253. doi:10.1109/TPEL.2014.2376474

[13] Huang Z., Wong S. C. and Tse C. K. Design methodology of a series-series inductive power transfer system for electric vehicle battery charger application. In: Energy

conversion congress and exposition (ECCE); Sep. 2014; Pittsburg, USA: IEEE; 2014. p. 1778–1782. doi:10.1109/ECCE.2014.6953633

[14] Qu X., Han H., Wong S. C., Tse C. K. and Chen W. Hybrid IPT topologies with constant current or constant voltage output for battery charging applications. IEEE Trans. Power Electron. 2015;30(11):6329–6337. doi:10.1109/TPEL.2015.2396471

[15] Zahid Z. U., Dalala Z. M., Zheng C., Chen R., Faraci W. E., Lai J.S.J., Lisi G. and Anderson D. Modeling and control of series–series compensated inductive power transfer system. IEEE J. Emerg Select Topics Power Electron. 2015;3(1):111–123. doi:10.1109/JESTPE.2014.2327959

[16] Buja G., Bertoluzzo M. and Mude K. N. Design and experimentation of wpt charger for electric city car. IEEE Trans. Ind. Electron. 2015;62(12):7436–7447. doi:10.1109/TIE.2015.2455524.

[17] Fincan B. and Ustun O. Limits and Solutions of Wireless Energy Transfer Systems. In: 7 ELECO International Conference on Electrical and Electronics Engineering; Dec. 2012; Bursa. Turkey: 8 2012. p. 455–459.

[18] Agcal A., Bekiroglu N. and Ozcira S. Examination of efficiency based on air gap and characteristic impedance variations for magnetic resonance coupling wireless energy transfer. J. Magn. 2015;20(1):57–61. doi:10.4283/JMAG.2015.20.1.057.

[19] Imura T. and Hori Y. Maximizing air gap and efficiency of magnetic resonant coupling for wireless power transfer using equivalent circuit and neumann formula. IEEE Trans. Ind. Electron. 2011;58(10):4746–4752. doi:10.1109/TIE.2011.2112317